Dynamics of field-induced polarization reversal in thin strained perovskite ferroelectric films with *c*-oriented polarization

Laurent Baudry,[1,*] Igor A. Luk'yanchuk,[2,3] and Anna Razumnaya[2,4]

[1]*Institut d'Electronique de Microélectronique et de Nanotechnologie, Département Hyperfréquences et Semiconducteurs, UMR CNRS 8520, Université des Sciences et Technologies de Lille Avenue Poincaré, BP 69, 59652 Villeneuve d'Ascq Cedex, France*

[2]*Laboratory of Condensed Matter Physics, University of Picardie, Amiens 80039, France*

[3]*L. D. Landau Institute for Theoretical Physics, Moscow, Russia*

[4]*Physics Department, Southern Federal University, Rostov on Don 344090, Russia*

(Received 24 March 2014; revised manuscript received 11 March 2015; published 21 April 2015)

The field-induced polarization reversal in the *c*-oriented ferroelectric phase of strained perovskite film has been studied. We show that in addition to the conventional longitudinal switching mechanism, when the *c*-oriented polarization vector changes its modulus, the longitudinal-transversal and transversal mechanisms when the perpendicular component of polarization is dynamically admixed are possible. The latter process can occur either via the straight-abrupt or initially continues polarization turnover scenario. We specified the obtained results for the case of $PbTiO_3$ and $BaTiO_3$ ferroelectrics and propose the experimental methods for their investigation.

DOI: 10.1103/PhysRevB.91.144110 PACS number(s): 77.80.bn, 77.55.Px, 77.80.Fm

I. INTRODUCTION

The ability of polarization switching in ferroelectric materials is essential for their application in memory-storage devices [1]. Meanwhile, the understanding of polarization reversal is the subject of controversies, partially related to the early assertion of Landauer [2] that the experimentally observed switching field is much smaller than the thermodynamic coercive field. To overcome this paradox it is commonly believed that the switching is inhomogeneous and domain-nucleation assisted [3]. Nonetheless, it was shown very recently [4] that homogeneous switching can be realized in ultrathin films of $PbTiO_3$ of thicknesses 2–6 nm and the Landauer conjecture is not as critical as thought.

The underlying mechanism of polarization reversal is of special interest for the mostly used pseudocubic perovskite crystals that, depending on the orientation of polarization $\mathbf{P} = (P_1, P_2, P_3)$, can exhibit tetragonal, orthorhombic, or rhombohedral structural phases in the ferroelectric state of the bulk material [5]. The situation is more diverse in the case of substrate-deposited perovskite ferroelectric films in which the substrate-provided deformation makes the lattice constant c in the z direction (perpendicular to the film surface) different from the in-plane lattice constants $a = b$ already in the high-temperature paraelectric phase with $\mathbf{P} = 0$.

In the present paper we report on a rotation mode of polarization reversal that can appear during the switching in strained perovskite films. We consider the most indicative homogeneous switching that can be tested experimentally using the setup of Ref. [4] and discuss the impact of this mode on the more complicated domain-provided switching in conclusion. We show that in addition to the conventional longitudinal switching mechanism, when the *c*-oriented polarization vector changes its modulus, the longitudinal-transversal and transversal mechanisms when the perpendicular component of polarization is dynamically admixed are possible.

II. THEORETICAL CONCEPTUAL FRAMEWORK AND RESULTS

To be more specific, we exploit the $PbTiO_3$ and $BaTiO_3$ substrate-clamped films, whose strain (u_m) - temperature (T) phase diagram contains at least four structural phases, as was first proposed by Pertsev, Zembilgotov, and Tagantsev [6,7] (see Fig. 1). The so-called *c* phase with $\mathbf{P} = (0,0,P_3)$ occurs at high compressive strains whereas the *aa* phase with $\mathbf{P} = (P_1,P_1,0)$ is realized at high tensile strains. Either the *ac* phase with $\mathbf{P} = (P_1,0,P_3)$ or the *r* phase with $\mathbf{P} = (P_1,P_1,P_3)$ can occur at low strains.

Considering the uniform polarization switching in $PbTiO_3$ and $BaTiO_3$ oxides we demonstrate that the situation is even more rich. Additional phases can dynamically appear during the polarization reversal. We restrict ourselves to the *c*-phase region of the u_m-T phase diagram and consider the switching process when the initially up-oriented polarization $\mathbf{P} = (0,0,P_3)$ decreases and then suddenly drops down under the oppositely applied field $\mathbf{E} = (0,0,E)$ with $E < 0$.

To describe the $PbTiO_3$ and $BaTiO_3$ materials we use the renormalized Landau-Devonshire free energy functionnal $\tilde{G}(\mathbf{P},E,T,u_m)$ given in Ref. [6], for which the account of the six-order terms is known to be important [8–10]:

$$\begin{aligned}\tilde{G}(\mathbf{P},E,T,u_m) &= a_1^*\left(P_1^2+P_2^2\right)+a_3^*P_3^2+a_{11}^*\left(P_1^4+P_2^4\right)\\ &+a_{33}^*P_3^4+a_{13}^*\left(P_1^2+P_2^2\right)P_3^2+a_{12}^*P_1^2P_2^2+a_{123}P_1^2P_2^2P_3^2\\ &+a_{112}\left[P_1^4\left(P_2^2+P_3^2\right)+P_3^4\left(P_1^2+P_2^2\right)+P_2^4\left(P_1^2+P_3^2\right)\right]\\ &+a_{111}\left(P_1^6+P_2^6+P_3^6\right)+\frac{u_m^2}{s_{11}+s_{12}}-EP_3. \qquad (1)\end{aligned}$$

The last term in Eq. (1) presents the field-driving interaction with the electric polarization. The renormalized coefficients a_1^*, a_3^*, a_{11}^*, a_{33}^*, a_{13}^*, and a_{12}^* depend on the misfit strain u_m

*laurent.baudry@iemn.univ-lille1.fr

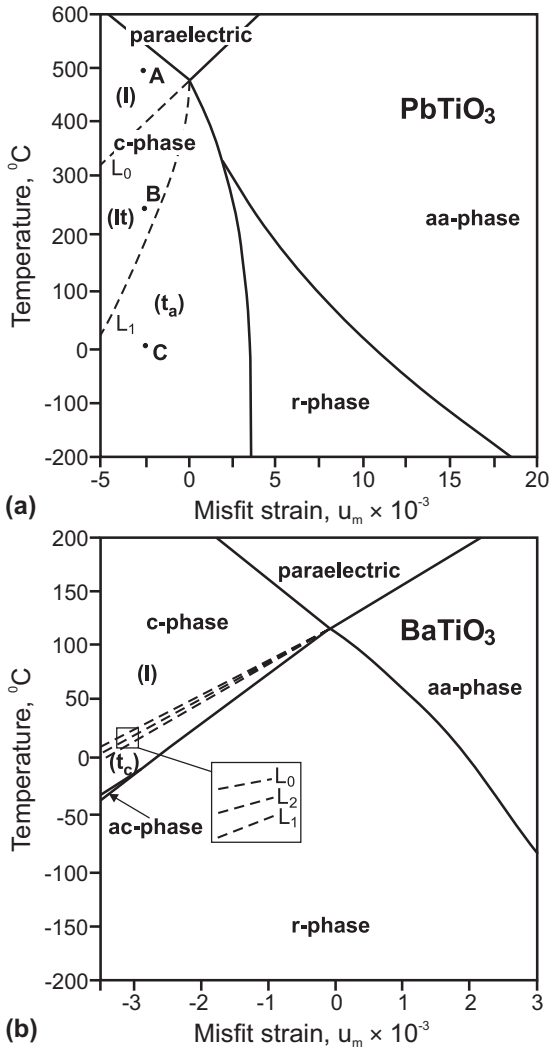

FIG. 1. Regions of the longitudinal l, longitudinal transversal lt, and transversal t switching regimes and corresponding separating lines L_0 and L_1 on the phase diagrams of strained films of (a) $PbTiO_3$ and (b) $BaTiO_3$, adopted from Refs. [6,7]. Line L_2 determines the type of transversal switching. The close location of L_2 and L_1 for $BaTiO_3$ implies that it occurs according the initially continuous turnover of polarization, t_c, whereas the absence of this line for $PbTiO_3$ means that transversal switching is straight abrupt t_a.

and temperature T whereas the other coefficients s_{11}, s_{12}, a_{111}, a_{112}, and a_{123} correspond to its bulk homologous, as was explicitly specified in Ref. [6]. We used the coefficients from Ref. [6] for $PbTiO_3$ and from Ref. [7] for $BaTiO_3$. Note that several alternative approaches were proposed to establish the u_m-T phase diagram of $BaTiO_3$ [11–14]. Their results are competitive with [6,7] mostly in the relative location of r and ac phases. This minor difference is not essential for our consideration and can be easily taken into account for each particular case; see Supplemental Material [15].

In what follows, we consider the competition between the switching-induced ac and r phases. By the substitution of the corresponding order parameters $\mathbf{P} = (P_1, 0, P_3)$ and $\mathbf{P} = (P_1, P_1, P_3)$ in Eq. (1) we obtain the following effective functional:

$$\tilde{G} = \frac{b_1}{2}P_1^2 + \frac{b_3}{2}P_3^2 + \frac{b_{11}}{4}P_1^4 + \frac{b_{33}}{4}P_3^4 + \frac{b_{13}}{2}P_1^2P_3^2 + \frac{b_{113}}{2}P_1^4P_3^2 + \frac{b_{133}}{2}P_1^2P_3^4 + \frac{b_{111}}{6}P_1^6 + \frac{b_{333}}{6}P_3^6 - EP_3, \tag{2}$$

where $b_1 = 2a_1^*$, $b_3 = 2a_3^*$, $b_{11} = 4a_{11}^*$, $b_{13} = 2a_{13}^*$, $b_{33} = 4a_{33}^*$, $b_{111} = 6a_{111}$, $b_{113} = 2a_{112}$, $b_{133} = 2a_{112}$, and $b_{333} = 6a_{111}$ for the ac-phase case, and $b_1 = 4a_1^*$, $b_3 = 2a_3^*$, $b_{11} = 8a_{11}^* + 4a_{12}^*$, $b_{13} = 4a_{13}^*$, $b_{33} = 4a_{33}^*$, $b_{111} = 12a_{111} + 12a_{112}$, $b_{113} = 2a_{123} + 4a_{112}$, $b_{133} = 4a_{112}$, and $b_{333} = 6a_{111}$ for the r-phase case.

Our approach is inspired by that given by Iwata and Ishibashi [16] for the case of a cubic (unstrained) lattice in the paraelectric phase. It was demonstrated that depending on the strength of the polarization-lattice coupling, two reversal mechanisms are possible. For strong cubic anisotropy the switching occurs like in a uniaxial one-component ferroelectrics by dynamical change of the modulus of the longitudinal polarization component P_3. For weak anisotropy the transient transversal component P_1 admixes to P_3 during the process. Such a *polarization-rotation* scenario can, for instance, occur in $PbZr_xTi_{1-x}O_3$ compounds when the anisotropic coupling is softened just as the composition parameter x approaches the morphotropic point $x \simeq 0.44$ from above. The microscopic simulation reveals also the rotational switching in the order-disorder cubic ferroelectric $KNbO_3$ [17].

The distinguishing feature of the substrate-deposited films from the bulk cubic case is the strain-induced uniaxial anisotropy that is reflected both by the splitting of the critical temperatures in the second order P_1^2 and P_3^2 terms and by accounting for the 6th-order cross-coupling terms. To understand the dynamical mechanism of polarization reversal we should catch the critical field at which the switching instability occurs. Application of an opposite electric field leads to the decrease of c-oriented polarization which stays yet positive until the critical field is reached. At this stage the field-driven polarization evolution $P_3(E)$ is given by the one-component variational equation:

$$\left(\frac{\partial \tilde{G}}{\partial P_3}\right)_{P_{1,2}=0} = b_3P_3 + b_{33}P_3^3 + b_{333}P_3^5 - E = 0. \tag{3}$$

The value of the critical field at which polarization switching starts can be obtained from the loss of the positive definiteness of the Hessian matrix $H_{ij} = \frac{\partial^2 \tilde{G}}{\partial P_i \partial P_j}$, presented in the extremal point of initial equilibrium $P_1 = 0$, $P_3 = P_3(E)$ as

$$H_{33} = b_3 + 3b_{33}P_3^2 + 5b_{333}P_3^4, \tag{4}$$

$$H_{11} = b_1 + b_{13}P_3^2 + b_{133}P_3^4, \tag{5}$$

$$H_{13} = H_{31} = 0, \tag{6}$$

where the dependence $P_3(E)$ is given by Eq. (3).

Upon longitudinal field E increases, the competition occurs between two instabilities of c-directed polarization P_3, the well-known longitudinal one $P_3^{(l)}$ and the transversal one $P_3^{(t)}$.

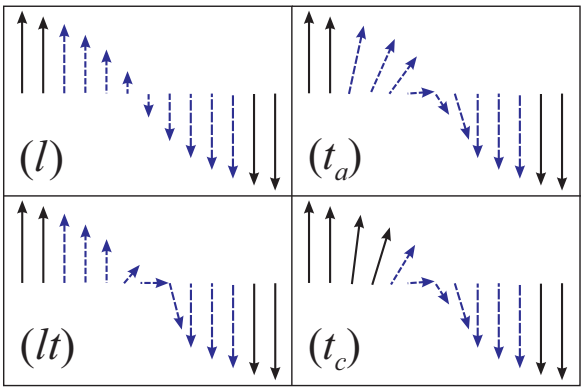

FIG. 2. (Color online) Reversal of the polarization vector as a function of the increasing with time switching electric field during longitudinal l, longitudinal transversal lt, transversal straight abrupt t_a, and transversal initially continuous t_c switching. Black solid lines present the thermodynamically stable field-induced states whereas the blue dashed lines present the transient states appearing during the abrupt switching process.

These instabilities, respectively, correspond to the longitudinal critical fields $E^{(l)}$ and $E^{(t)}$, determined by the conditions $H_{33}(P_3(E^{(l)})) = 0$ and $H_{11}(P_3(E^{(t)})) = 0$. Importantly, the switching occurs at the instability field $E^{(l)}$ or $E^{(t)}$ which is attained first and the further scenario of polarization vector evolution is determined by the occurring type of instability.

(i) For $|E^{(l)}| < |E^{(t)}|$ the *longitudinal l* switching instability is realized first and the polarization vector reverses its direction by a change of the amplitude of P_3 from positive to negative, passing through $P_3 = 0$.

(ii) For $|E^{(t)}| < |E^{(l)}|$ the *transversal t* switching instability is realized first and the component P_1 is admixed to P_3 after the beginning of the reversal process, just above $E^{(t)}$. Polarization switching has, therefore, the rotational constituent, like in the Iwata and Ishibashi model. The smaller value of $|E^{(t)}|$ mitigates the paradox of the coercive field (usually calculated at $|E^{(l)}|$).

(iii) There can exist also the mixed *longitudinal-transversal lt* regime when the polarization reversal starts according to the longitudinal scenario at $E = E^{(l)}$ but the transient transversal component P_1 appears at the later stage of the process.

The polarization evolution in l, lt, and t switching regimes is sketched in Fig. 2. We presume that they are separated by crossover lines L_0 and L_1 in the u_m-T phase diagram and find the condition of their existence. The t-type switching can have either *initially continuous* t_c or *straight-abrupt* t_a character as will be specified later.

According to the given above consideration the transversal component P_1 can dynamically admix to the component P_3 during polarization reversal if the polarization-dependent Hessian matrix element H_{11} becomes negative in the course of the switching. This occurs, e.g., when coefficient b_1 is negative. Then, when the dropping-down polarization goes through the state with vanishing P_3, the element H_{11}, according Eq. (5), acquires the negative sign in the vicinity of $P_3 = 0$. The polarization vector will experience the instability towards the transversal deviation and the lt regime will be realized. Therefore the crossover line L_0 between l and lt regimes is given by the condition:

$$L_0 : b_1(u_m, T) = 0. \tag{7}$$

Noteworthy is that the line L_0 can be found in the u_m-T phase diagram as the prolongation of the paraelectric aa-phase transition line located in the $u_m > 0$ region into the $u_m < 0$ region.

The condition of crossover between lt and t switching regimes can be found by equating the critical fields $E^{(l)}$ and $E^{(t)}$ or, what is equivalent and easier, by equating the corresponding longitudinal and transversal critical polarizations $P_3^{(l)} = P_3(E^{(l)})$ and $P_3^{(t)} = P_3(E^{(t)})$ calculated at these fields. The latter can be found from Eqs. $H_{33}(P_3^{(l)}) = 0$ and $H_{33}(P_3^{(t)}) = 0$ as

$$P_3^{(l)2} = \frac{\left(9b_{33}^2 - 20b_3b_{333}\right)^{1/2} - 3b_{33}}{10b_{333}}, \tag{8}$$

$$P_3^{(t)2} = \frac{\left(b_{13}^2 - 4b_1b_{133}\right)^{1/2} - b_{13}}{2b_{133}}. \tag{9}$$

Condition $P_3^{(l)} = P_3^{(t)}$ determines the crossover line L_1 between lt and t regimes:

$$L_1: \frac{b_3b_{13} - 3b_1b_{33}}{5b_1b_{333} - b_3b_{133}} = \frac{5b_1b_{333} - b_3b_{133}}{3b_{33}b_{133} - 5b_{13}b_{333}}. \tag{10}$$

We delimit now the location of l, lt, and t switching regimes and corresponding crossover lines L_0 and L_1 on the phase diagram of strained $PbTiO_3$ and $BaTiO_3$ films using the taken from [6] strain and temperature dependencies of coefficients of the functional (2) and examining separately the cases of transitions through the ac and r phases.

In the case of $PbTiO_3$ all these regimes are clearly visible and are located inside the region of thermodynamically stable c phase as shown in Fig. 1(a). To study the transient polarization dynamics we select the representative points for each transition region [points A, B, and C in Fig. 1(a)] and numerically solve the Landau-Khalatnikov kinetic equations,

$$L_i \frac{dP_i}{dt} = -\frac{\delta \tilde{G}}{\delta P_i}, \tag{11}$$

for each polarization component $P_i = P_i(t)$. Here L_i are the corresponding damping coefficients. The results are presented in Fig. 3 in the form of experimentally measurable longitudinal and transversal polarization currents $I_l = \frac{dP_3}{dt}$ and $I_t = \frac{dP_1}{dt}$.

Point A is selected for the l-switching region at $u_m = -0.0025$ and $T = 500\,^{\circ}$C. As it follows from Fig. 3(a) the polarization current has only the longitudinal component that is characteristic for the longitudinal switching regime. Point B corresponds to the lt-switching region and is taken at $u_m = -0.0025$ and $T = 250\,^{\circ}$C. As shown in Fig. 3(b) both components of the polarization current are observed, but the transversal one is excited after the longitudinal one and vanishes earlier than the longitudinal one. Point C is taken in the t-switching region at $u_m = -0.0025$ and $T = 0\,^{\circ}$C. As shown in Fig. 3(c) the longitudinal and transversal polarization currents are excited simultaneously.

In the case of $BaTiO_3$ [Fig. 1(b)] one can observe only the l- and t-switching regimes. The lt-switching regime is difficult

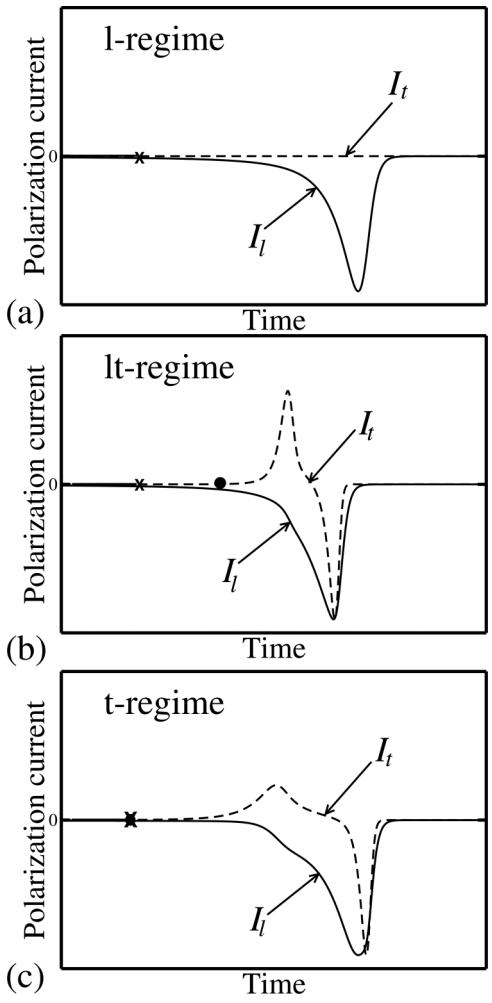

FIG. 3. Time dependence of the longitudinal, $I_l = \frac{dP_3}{dt}$, and transversal, $I_t = \frac{dP_1}{dt}$, polarization currents for (a) transversal t, (b) longitudinal transversal lt, and (c) longitudinal l switching regimes for $PbTiO_3$. Panels (a)–(c) correspond to the points A, B, and C in Fig. 1(a). The cross and circle markers indicate the beginning of the longitudinal and transversal polarization reversal processes correspondingly.

to detect because of the very close location of the lines L_0 and L_1.

An important issue for the t-type switching is the dynamical behavior of polarization just upon reaching the transversal instability field. Under certain conditions the intermediately stable ac or r phase can be induced just above $E^{(t)}$. Then, the continuous (as function of the field) turnover of polarization through this phase will precede the abrupt rotational drop-down. To distinguish between the shown in Fig. 2 initially continuous t_c and straight-abrupt t_a transversal switching processes we study the global stability of the functional (2) with respect to small deviations ΔP_1, ΔP_3 about the equilibrium point $P_1^{(t)} = 0$ and $P_3^{(t)} = P_3(E^{(t)})$ exactly at $E = E^{(t)}$. This is a peculiar problem since at $E = E^{(t)}$ the coefficient H_{11} before $(\Delta P_1)^2$ is equal to zero and the higher-order terms should be taken into account. Following the catastrophe theory we keep only the most relevant terms and present the expansion of (2) as

$$\tilde{G} \approx \tfrac{1}{2}\rho(\Delta P_3)^2 + \mu(\Delta P_3)(\Delta P_1)^2 + \tfrac{1}{2}\lambda(\Delta P_1)^4, \qquad (12)$$

where $\rho = H_{33}$ [see (5)], $\mu = \frac{1}{2}\frac{\partial^3 \tilde{G}}{\partial P_3 \partial P_1^2} = b_{13}P_3^{(t)} + 2b_{133}P_3^{(t)3}$, and $\lambda = \frac{1}{12}\frac{\partial^4 \tilde{G}}{\partial P_1^4} = \frac{1}{2}b_{33}$. Transformation $x = (\Delta P_1)^2$ and $z = (\Delta P_3)$ map the problem onto the study of the quadratic functional $\frac{1}{2}\lambda x^2 + \mu xy + \frac{1}{2}\rho y^2$. The last one is globally unstable at $\lambda\rho > \mu^2$ that provides the straight-abrupt switching at $E \gtrsim E^{(t)}$. At $\lambda\rho < \mu^2$ this functional is locally stable and at the initial stage of the reversal process the P_1 component develops continuously as a function of the field. Using the given above definition of λ, ρ, μ and excluding $P_3^{(t)}$ according Eq. (9) we, after some algebra, present the line L_2, separating these two regimes on the u_m-T phase diagram by equation,

$$L_2 : PR = Q^2, \qquad (13)$$

with

$$\begin{aligned} P &= b_3 b_{33} b_{13} - 3b_1 b_{33}^2 + 2b_1 b_{13}^2 - 8b_1^2 b_{133}, \\ Q &= 5b_1 b_{33} b_{333} - b_3 b_{33} b_{133}, \\ R &= 3b_{33}^2 b_{133} - 2b_{13}^2 b_{133} + 8b_1 b_{133}^2 - 5b_{13} b_{33} b_{333}. \end{aligned} \qquad (14)$$

The t_c and t_a switching regions are located below and above this line correspondingly.

Thoughtful analysis of the equation (13) for the $BaTiO_3$ case shows that the line L_2 is located very close to the line L_1 [see Fig. 1(b)] which means that "t_c switching" always occurs through the intermediate field-induced ac phase. In contrast, the line L_2 does not exist in c-phase region of the phase diagram of $PbTiO_3$ [Fig. 1(a)] which implies the "t_a switching" through the intermediate r phase takes place. Note that the maximal value of the transient transversal polarization component depends on location on the u_m-T diagram and varies from zero, close to the L_0, L_1, L_2 lines, to almost 0.4–0.5 of P_3 at $E = 0$, close to c-ac transition line. The situation is similar in $PbTiO_3$.

III. CONCLUSIONS

We have demonstrated the existence of different homogeneous switching regimes in strained thin ferroelectric films of $PbTiO_3$ and $BaTiO_3$. Depending on the temperature and on the misfit strain, one can distinguish the polarization reversal, governed by the longitudinal, transversal, or mixed longitudinal-transversal switching regimes. All three mechanisms can be observed in $PbTiO_3$ compounds. In $BaTiO_3$ compounds only the longitudinal and transversal mechanisms can be detected. The latter occurs through the intermediate ac phase with initial continuous turnover of the polarization vector as a function of the field. The dynamic appearance of the transversal polarization during the homogeneous transition can be observed by the time-resolved piezoforce microscopy or by the in-field Raman spectroscopy sensitive to the polarization vector variation, using the setup of Ref. [4] for realization of homogeneous switching.

The described rotational mode can also be relevant for inhomogeneous switching by the formation of vortexlike nucleation domains with a circulated transversal polarization

component [18,19]. The situation can be even more complicated if the periodic Kittel structure of 180° ferroelectric domains exist in the initial *c* phase or/and 90° transversal ferroelastic stripe domains emerge during the switching process. Study of such scenarios on the basis of the presented above calculations is in progress.

ACKNOWLEDGMENT

This work was supported by EC-FP7 ITN-NOTEDEV and IRSES-SIMTECH mobility programs and by the RSF, Grant No. 14-12-00258.

[1] J. F. Scott, *Ferroelectric Memories*, Springer Series in Advanced Microelectronics (Springer, Berlin, 2000).
[2] R. Landauer, J. Appl. Phys. **28**, 227 (1957).
[3] A. K. Tagantsev, L. E. Cross, and J. Fousek, *Domains in Ferroic Crystals and Thin Films* (Springer, New York, 2010).
[4] M. J. Highland, T. T. Fister, M.-I. Richard, D. D. Fong, P. H. Fuoss, C. Thompson, J. A. Eastman, S. K. Streiffer, and G. B. Stephenson, Phys. Rev. Lett. **105**, 167601 (2010).
[5] M. E. Lines and A. M. Glass, *Principles and Applications of Ferroelectrics and Related Materials* (Oxford University Press, Oxford, 1977).
[6] N. A. Pertsev, A. G. Zembilgotov, and A. K. Tagantsev, Phys. Rev. Lett. **80**, 1988 (1998).
[7] N. A. Pertsev, A. G. Zembilgotov, and A. K. Tagantsev, Ferroelectrics **223**, 79 (1999).
[8] A. J. Bell and L. E. Cross, Ferroelectrics **59**, 197 (2011).
[9] Y. L. Li, L. E. Cross, and L. Q. Chen, J. Appl. Phys. **98**, 064101 (2005).
[10] Y. L. Wang, A. K. Tagantsev, D. Damjanovic, N. Setter, V.K. Yarmarkin, A. I. Sokolov, and I. A. Lukyanchuk, J. Appl. Phys. **101**, 104115 (2007).
[11] O. Diéguez, S. Tinte, A. Antons, C. Bungaro, J. B. Neaton, K. M. Rabe, and D. Vanderbilt, Phys. Rev. B **69**, 212101 (2004).
[12] B.-K. Lai, I. A. Kornev, L. Bellaiche, and G. J. Salamo, Appl. Phys. Lett. **86**, (2005).
[13] V. B. Shirokov, Yu. I. Yuzyuk, B. Dkhil, and V. V. Lemanov, Phys. Rev. B **75**, 224116 (2007).
[14] A. Kvasov and A. K. Tagantsev, Phys. Rev. B **87**, 184101 (2013).
[15] See Supplemental Material at http://link.aps.org/supplemental/10.1103/PhysRevB.91.144110 where we demonstrate the location of lines L_0, L_1, and L_2 at the phase diagram of $BaTiO_3$ for alternative choices of coefficients in the functional [Eq. (1)] given in Refs. [6,14].
[16] M. Iwata and Y. Ishibashi, Jpn. J. Appl. Phys. **38**, 5670 (1999).
[17] S. R. Phillpot, M. Sepliarsky, M. G. Stachiotti, R. L. Migoni, and S. K. Streiffer, J. Mat. Science. Phys. **40**, 3213 (2005).
[18] L. Baudry, I. Luk'yanchuk, and A. Sené, Ferroelectrics **427**, 34 (2012).
[19] L. Baudry, A. Sené, I. A. Luk'yanchuk, L. Lahoche, and J. F. Scott, Phys. Rev. B **90**, 024102 (2014).